PHYSICAL REVIEW B **86**, 060514(R) (2012)

Skyrmionic state and stable half-quantum vortices in chiral *p*-wave superconductors

Julien Garaud and Egor Babaev
Department of Physics, University of Massachusetts, Amherst, Massachusetts 01003, USA, and
Department of Theoretical Physics, The Royal Institute of Technology, Stockholm SE-10691, Sweden

(Received 13 January 2012; published 29 August 2012)

Observability of half-quantum vortices and skyrmions in *p*-wave superconductors is an outstanding open question. Under the most common conditions, fractional flux vortices are not thermodynamically stable in bulk samples. Here we show that in chiral *p*-wave superconductors, there is a regime where, in contrast, lattices of integer-flux vortices are not thermodynamically stable. Instead, skyrmions made of spatially separated half-quantum vortices are the topological defects produced by an applied external field.

DOI: 10.1103/PhysRevB.86.060514 PACS number(s): 74.25.Ha, 74.20.Rp, 74.25.Dw

Higher broken symmetries in *p*-wave superconductors have inspired longstanding interest to realize topological defects more complicated than vortices. Much of the early discussions of various complex topological defects were in the context of superfluid ^{3}He.[1] Recently attention to these questions has raised dramatically in connection with superconductors which are argued to have *p*-wave pairing, such as Sr_2RuO_4. The highly interesting possibility there is connected with half-quantum vortices.[2–8] Their statistics is non-Abelian and they could potentially be used for quantum computations.[9] Other kinds of topological defects discussed in connection with spin-triplet superconductors are skyrmions[10] and hopfions.[11] In superconducting materials, the creation of these topological excitations is highly nontrivial. Superconducting components are coupled by a gauge field and there are also symmetry-reducing intercomponent interactions. As a consequence, fractional vortices have logarithmically or linearly divergent energies (see, e.g., Ref. 8), while integer-flux vortices have finite energy per unit length. Consequently, under usual conditions, half-quantum vortices are thermodynamically unstable in bulk systems. It was argued that complex setups, such as mesoscopic samples, are needed for their creation.[2,8,12] Recently it was claimed that a half-quantum vortex was observed in a mesoscopic sample of Sr_2RuO_4.[2] Other proposed routes to observe fractional vortices invoke (i) thermal deconfinement,[3,6,13] (ii) potential materials with strongly reduced spin stiffness,[4] and (iii) regimes very close to the upper critical magnetic field, where gauge-field mediated half-quantum vortex confinement is weak.[5] In some more general systems it was shown that fractional vortices could be thermodynamically stable near boundaries.[14] Today the conditions under which half-quanta vortices and skyrmions[10] could be experimentally created in bulk superconductors still remains an outstanding open question.

In this Rapid Communication we investigate the magnetic response of the Ginzburg-Landau model that has been widely applied to Sr_2RuO_4.[15,16] Our considerations apply to two-dimensional systems or three-dimensional problems with translation invariance along the z direction. Then the free energy density reads

$$\mathcal{F}(\psi_a,\boldsymbol{A}) = |\nabla\times\boldsymbol{A}|^2 \tag{1a}$$

$$+|D_x\psi_1|^2+|D_y\psi_2|^2+\gamma|D_y\psi_1|^2+\gamma|D_x\psi_2|^2 + 2\gamma\,\mathrm{Re}[(D_x\psi_1)^*D_y\psi_2+(D_y\psi_1)^*D_x\psi_2] \tag{1b}$$

$$+(2\gamma-1)|\psi_1|^2|\psi_2|^2+\sum_{a=1,2}-|\psi_a|^2+\frac{1}{2}|\psi_a|^4 \tag{1c}$$

$$+\gamma|\psi_1|^2|\psi_2|^2\cos[2(\varphi_2-\varphi_1)]. \tag{1d}$$

The different components of the order parameter are denoted $\psi_{1,2}=|\psi_{1,2}|e^{i\varphi_{1,2}}$; $\boldsymbol{D}=\nabla+ie\boldsymbol{A}$. The *p*-wave state is described here by a doublet of complex fields subjected to the following symmetry breaking coupling: $\mathrm{Re}(\psi_1^{*2}\psi_2^2)=|\psi_1|^2|\psi_2|^2\cos[2(\varphi_2-\varphi_1)]$. The ground state breaks the $U(1)\times\mathbb{Z}_2$ symmetry, since the ground state phase difference $(\varphi_2-\varphi_1)$ is either $\pi/2$ or $3\pi/2$. Gradient terms (1b) make this model clearly anisotropic in the xy plane. The coefficient γ, controlling the anisotropy, should be $\gamma>1/3$ for Sr_2RuO_4, according to Ref. 15. The coupling constant e is a convenient quantity to parametrize the penetration depth of the magnetic field. The discrete $\mathbb{Z}_2$ symmetry dictates that the system allows domain-wall solutions interpolating between two regions with different phase locking. Such domain walls are energetically expensive and thus are not intrinsically stable. It was suggested that they could be observable if pinned by crystalline defects.[18] Also domain walls formed as dynamic excitations inside vortex lattices were studied extensively in Ref. 19. They could be experimentally observable in these setups since they pin half-quantum vortices.[18,19]

Returning to the discussion of vortices, one can observe that the system (1) has $U(1)\times\mathbb{Z}_2$ broken symmetry. Thus a single half-quantum vortex (with winding only in one of the phases) has a linearly diverging energy and thus is not thermodynamically stable.[8] Also from this broken symmetry, the existence of skyrmionic excitations would not follow. The previous works required higher broken symmetry for the existence of skyrmions.[10] However, we show below that there is a considerable window of parameters where the system (1) possesses what we term a "skyrmionic phase." In that phase, mostly because of favorable competition between field gradients, and potential and magnetic energies, the system does have *thermodynamically stable* skyrmions while ordinary integer-flux vortex lattices are *not* thermodynamically stable. These skyrmions are bound states of spatially separated half-quanta vortices, connected by domain walls. Half-quantum vortices are linearly confined into integer vortices in a bulk sample because of the terms $|\psi_1|^2|\psi_2|^2\cos[2(\varphi_2-\varphi_1)]$. However, on a (closed) domain wall, a composite vortex

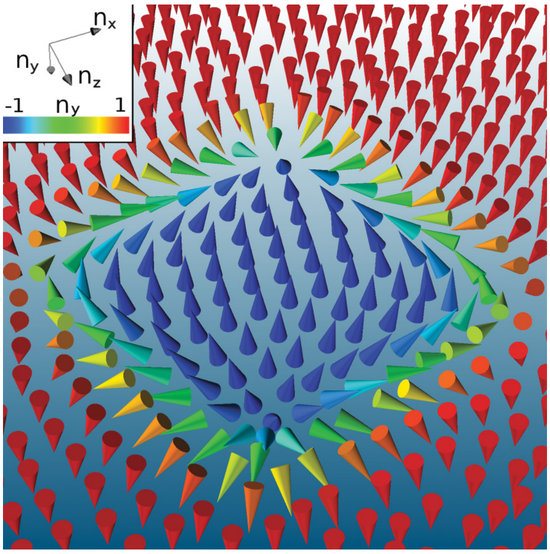

FIG. 1. (Color online) Numerically calculated texture of the pseudospin vector for a skyrmion carrying a topological charge $\mathcal{Q} = 2$. As can be seen in the picture the skyrmionic topological charge density is confined in a closed domain wall.

should split along this wall, since the above-mentioned term has unfavorable values of the phase difference. Indeed, such deconfining allows to reduce energetically unfavorable values of the phase differences. Because of this vortex splitting and the resulting repulsive interactions, vortices trapped on the domain wall can prevent the collapse of a closed domain wall. The main result of this Rapid Communication is that we show that these objects are characterized by an integer-valued skyrmionic topological charge and that they can be energetically cheaper than vortices. Such a skyrmion is displayed in Fig. 1 as a texture of a pseudospin vector field defined later on.

We investigated structures carrying N flux quanta (i.e., with each phase winding $\oint \nabla\varphi_a = 2\pi N$) as functions of the gauge coupling e and the anisotropy parameter γ. Ground states, carrying a given number of magnetic flux quanta, are computed numerically by minimizing the energy within a finite element framework provided by the FREEFEM++ library.[20] See technical details in the Supplemental Material.[17]

We find that if the penetration length is sufficiently large (i.e., at small values of the coupling constant e), the system indeed forms ordinary Abrikosov vortices in an external field. On the other hand, for sufficiently large e the system behaves as a type-I superconductor. However, there is a regime in a wide range of intermediate coupling constants e, where integer-flux vortices are more expensive than bound states of spatially separated half-quantum vortices connected by a closed domain wall. Such configurations carrying different numbers of flux quanta are given in Figs. 2–4. The clearly visible preferred directions for supercurrents originate in the anisotropies (1b). The cores in different components do not coincide in space. This means fractionalization of vortices in this state. Each of the split cores carries half of a flux quantum (for detailed calculations of fractional vortices flux quantization, see, e.g., Ref. 8).

The configurations found here are actually skyrmions, although it may not be obvious from Figs. 2–4. To prove

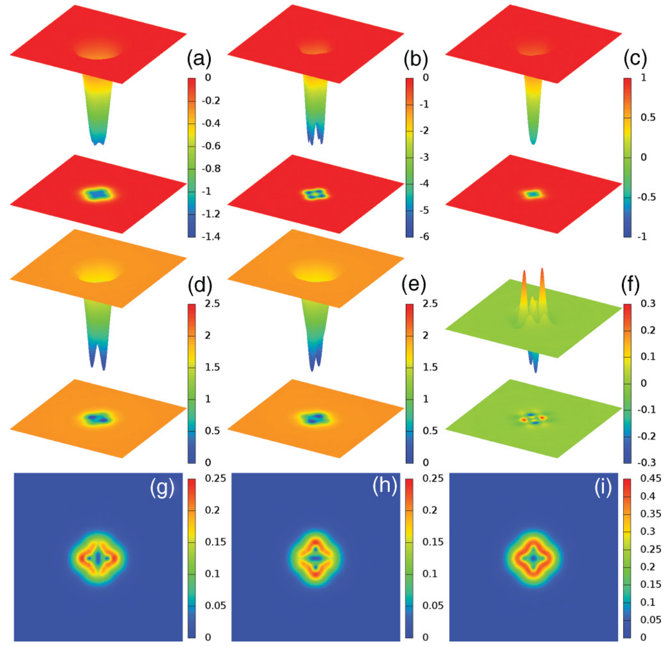

FIG. 2. (Color online) A thermodynamically stable skyrmion carrying two flux quanta, with $e = 0.8$ and $\gamma = 0.5$. Displayed quantities are magnetic flux (a), the (inverted) energy density (b), and the sine of the phase difference $\sin(\varphi_2 - \varphi_1)$ (c). On the second line, the densities of the superconducting order parameter components $|\psi_1|^2$ (d), $|\psi_2|^2$ (e), and the "doubled phase difference" $\mathrm{Im}(\psi_1^{*\,2}\psi_2^2)$ (f) are shown. (g) and (respectively h) on the third line are the supercurrents associated with each component ψ_1 (respectively ψ_2) of the order parameter (Ref. 17). (i) shows the total supercurrent.

that the solutions are skyrmions the two-component model (1) is mapped to an anisotropic nonlinear σ model.[21] In that mapping the superconducting condensates are projected on the Pauli matrices $\boldsymbol{\sigma}$, allowing to define the pseudospin vector $\mathbf{n}$:

$$\mathbf{n} \equiv (n_x,n_y,n_z) = \frac{\Psi^\dagger \boldsymbol{\sigma} \Psi}{\Psi^\dagger \Psi} \quad \text{where} \quad \Psi^\dagger = (\psi_1^*,\psi_2^*). \tag{2}$$

The target space being a sphere, together with the one-point compactification of the plane, defines the map $\mathbf{n} : S^2 \to S^2$. Such maps are classified by the homotopy class $\pi_2(S^2) \in \mathbb{Z}$, so there exists an integer valued topological charge

$$\mathcal{Q}(\mathbf{n}) = \frac{1}{4\pi} \int_{\mathbb{R}^2} \mathbf{n} \cdot \partial_x \mathbf{n} \times \partial_y \mathbf{n}\, dxdy. \tag{3}$$

For a skyrmion, $\mathcal{Q} = N$, while $\mathcal{Q} = 0$ for ordinary vortices. The terms in (1c) and (1d) break the $O(3)$ symmetry of the pseudospin $\mathbf{n}$ down to $\mathbb{Z}_2$. In a nonlinear σ model, such anisotropy would undermine the stability of the skyrmions. However, this collapse does not occur in the Ginzburg-Landau model, because of the behavior of the gradient energy, which is demonstrated below.

The numerically computed topological charge (3) is found to be an integer (with a negligible relative error of the order 10^{-5}, due to the discretization) for the closed domain wall/vortex systems which are therefore skyrmions. The solutions shown in Figs. 2–4 have a skyrmionic topological charge $\mathcal{Q} = 2$, $\mathcal{Q} = 5$, and $\mathcal{Q} = 8$, correspondingly. The terminology skyrmion is more intuitively obvious when the

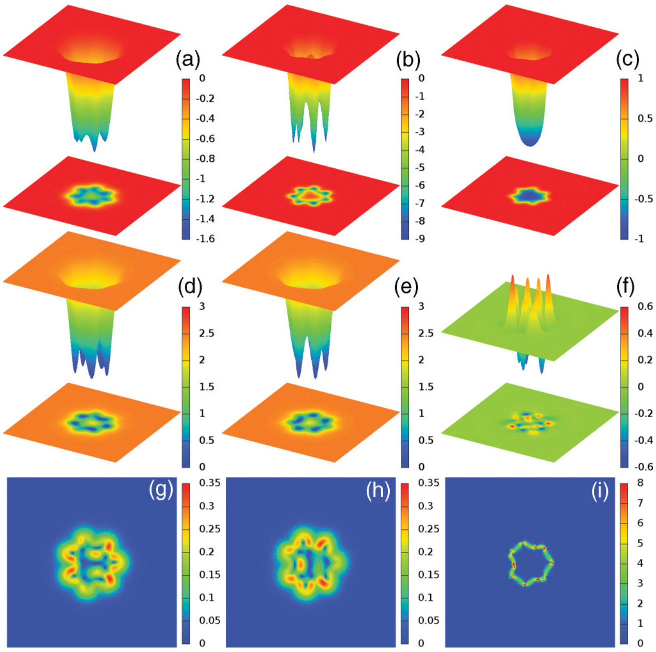

FIG. 3. (Color online) A skyrmion carrying five flux quanta, with $e = 0.8$ and $\gamma = 0.4$. Displayed quantities are the same as in Fig. 2, except (i) shows the gradient of the phase difference $\nabla(\varphi_{12})$, which is nonzero at the domain wall. The skyrmion consists of ten spatially separated half-quantum vortices. It assumes a complicated nonsymmetric structure due to a competition of a preferred geometry of a skyrmion with the anisotropies [Eq. (1b)].

solutions are represented in terms of the pseudospin vector field $\mathbf{n}$, as in Fig. 1. However, unlike skyrmions in a nonlinear σ model, here the skyrmionic topological charge density is mostly concentrated on the half-quantum vortices and on the domain wall.

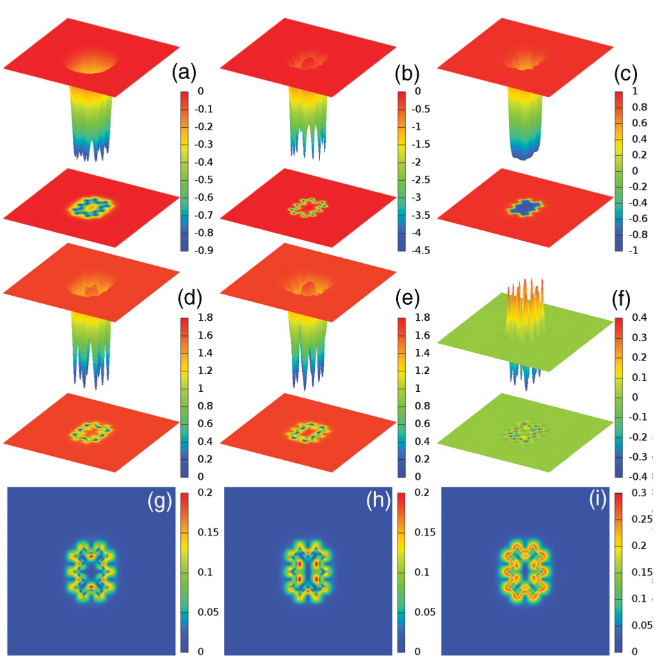

FIG. 4. (Color online) A skyrmion with $N = 8$, $e = 0.6$, and in the case of higher anisotropy, $\gamma = 0.6$. Displayed quantities are the same as in Fig. 2.

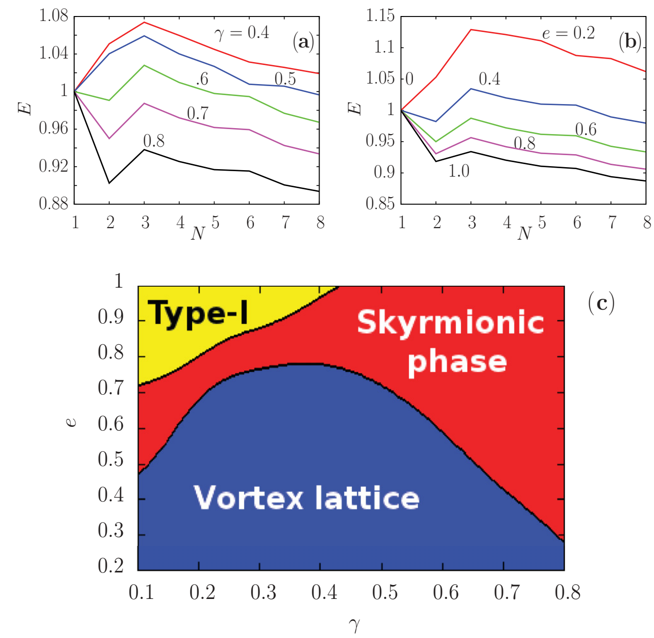

FIG. 5. (Color online) The upper panels show the dependence of the energy per flux quantum for skyrmions of different topological charges $\mathcal{Q}$ (values are given in the units of the energy of one integer-flux vortex). The $N = 1$ point at the origin corresponds to an ordinary vortex solution. (a) shows calculations corresponding to different γ for fixed $e = 0.6$, while (b) displays how the energy per flux quantum changes with e and N for a fixed anisotropy parameter $\gamma = 0.7$. The $\mathcal{Q} = 2$ skyrmions are usually less energetically expensive than the $\mathcal{Q} = 3$. This is because the $\mathcal{Q} = 2$ skyrmions can be better aligned with the underlying anisotropies, than the $\mathcal{Q} = 3$ skyrmions. The lower panel displays the *phase diagram*, calculated using energy characteristics of $\mathcal{Q} = 5$ skyrmions. The different colors refer to different physical properties. The type-I region is shown by a yellow shade. The lower part of the phase diagram shows regions where skyrmions (red) or vortex lattices (blue) form in an applied external field. The phase diagram retains a similar structure in calculations with different topological charges. With the increase of the skyrmionic charge $\mathcal{Q}$, the region where skyrmions are energetically preferred over vortex lattices grows slightly. These results apply either for two-dimensional systems or three-dimensional systems with translational invariance along the z axis. In the latter case the energy should be understood as the energy per unit length of a skyrmion line (i.e., a skyrmion texture in the xy plane which is invariant under translation along the z axis). The discretization errors can be estimated by computing the total magnetic flux and comparing it to the exact value which follows from the quantization condition $2\pi N/e$. This gives the relative accuracy on the flux to be around 10^{-5}. From that, the accuracy on the energy is estimated to be at least three orders of magnitude smaller than the energy difference between skyrmions and vortices.

The main result of this work is that skyrmions of the above type (and thus half-quantum vortices) can be *less energetic* than integer-flux ordinary vortices and *thermodynamically stable* in the chiral p-wave superconductors. The critical external magnetic field H_{c1} for the formation of a flux-carrying topological defect is determined by the condition where the Gibbs free energy $G = E_d - 2\int \mathbf{B}\cdot\mathbf{H}_e\, dxdy$ becomes negative. Here E_d and $\mathbf{B}$ are the energy and magnetic field of

TABLE I. Different contributions to the skyrmion energy *per flux quantum*. $\mathcal{Q} = 5$ skyrmions are considered in this example. The results are compared with the contributions to the energy of a single vortex (which determines the lower bound on vortex lattice energy near the first critical magnetic field H_{c1}). The gradient contribution $E_{\rm grad}$ is given by the integrated (1b), and the magnetic energy $E_{\rm mag}$ by (1a). The potential energy $E_{\rm pot}$ is (1c) and $E_{\mathbb{Z}_2}$ is (1d). The first block, for which $\gamma = 0.8$ and $e = 0.4$, corresponds to the state where skyrmions are thermodynamically stable but vortex lattices are not. The second block is for $\gamma = 0.6$ and $e = 0.2$. It corresponds to a regime with a standard Abrikosov vortex lattice. Here the skyrmions are local minima of the free energy functional. They are more expensive than vortices but, if formed, they are protected against decay by a finite energy barrier. In the second example the win in the kinetic energy is too small to overcome the extra energy cost associated with domain-wall formation and magnetic energy.

	$E_{\rm total}$	$E_{\rm grad}$	$E_{\rm pot}$	$E_{\mathbb{Z}_2}$	$E_{\rm mag}$
Vortex	19.7759	10.7518	−12.0190	16.5195	4.5235
Skyrm.	18.9004	8.10522	−12.2301	17.6336	5.3916
Vortex	32.1684	19.3227	−19.0381	25.4445	6.4392
Skyrm.	37.6456	16.2529	−22.1474	32.8582	10.6818

the defect. $\mathbf{H}_e$ denotes the applied field. Thus $H_{c1} = E_d/2\Phi$ where Φ is the magnetic flux produced by the defect. The defects are thermodynamically stable if the critical external magnetic field's energy density H_{c1}^2 is smaller than the condensation energy. We investigated the energy dependence of the skyrmions on the number of enclosed flux quanta N. The energy of an integer-flux vortex is used as a reference point. As shown in Figs. 5(a) and 5(b), for low N, the energy depends nonmonotonically on N. This is because the preferred symmetry of small N configurations in some cases is in strong conflict with the anisotropies of the model. In the large-N limit the energy per flux quantum gradually tends to some value. The main point here is that the energy per flux quantum for skyrmions is in certain cases smaller than that of vortices. This signals instability of vortex lattices with respect to skyrmion formation.

Next, the thermodynamical stability of skyrmions is investigated. Results for $N = 5$ quanta are reported as a characteristic example in Fig. 5(c). We find that there are three regimes on the resulting phase diagram. When the penetration length is large (i.e., low e), the system shows the usual type-II superconductivity. When the penetration length is small, the system is a type-I superconductor. For intermediate values of the penetration length, depending on the underlying anisotropies γ, the external field produces skyrmions rather than vortex lattices. To understand the instability of vortex lattices with respect to skyrmion formation, different contributions to energy are investigated in Table I. In the skyrmionic state, vortex lattice decay into skyrmions is driven by a win in gradient and potential energies although there is a loss in magnetic energy as well as the extra cost of producing a domain wall.

The skyrmions we find are structurally different from skyrmions discussed in other kinds of superconductors[10] because of the different symmetry of the model. Another principal difference is the nature of the skyrmionic state, namely, Ref. 10 proposed models where there are only skyrmionic solutions carrying two flux quanta, with the latter forming stable lattices. In contrast, the model we consider supports skyrmions with any integer value of topological charge. Importantly, the energy per flux quantum here is a sublinear function of the topological charge, which prohibits a ground state in the form of a lattice of the simplest skyrmions envisaged in Ref. 10. Instead our model predicts more complicated high-topological-charge skyrmionic structures. Also in a type-II regime our model predicts metastable states of coexisting vortices and skyrmions.

In conclusion, we have shown that the phase diagram of chiral p-wave superconductors has a thermodynamically stable skyrmionic phase between type-I and the usual type-II regimes. This is despite the fact that the model has $U(1) \times \mathbb{Z}_2$ broken symmetry where naive symmetry arguments would rule out skyrmionic excitations. In the skyrmionic phase, the long-sought-after half-quantum vortices acquire thermodynamic stability. These objects can be detected with surface probes through their characteristic profile of the magnetic field. The phase transition into a skyrmionic state should be first order, because the energy per flux quantum is decreasing with the skyrmionic topological charge.

The possibly chiral superconductor Sr_2RuO_4 which is frequently described by the model (1) may have a penetration length which is slightly too large to fall into the skyrmionic phase. However, in this case the model predicts metastable skyrmionic excitations (which are slightly more energetic than vortices). Recently sporadic formation of objects with multiple flux quanta were reported in Fig. 2 of Ref. 22. Higher resolution scans of the magnetic field profile could confirm or rule out if the observed objects are skyrmions. Another scenario for flux clustering in this material is type-1.5 superconductivity which can arise if to take into account its multi-band nature.[23]

We thank Daniel Agterberg and Johan Carlström for discussions. The work is supported by the Swedish Research Council, and by the Knut and Alice Wallenberg Foundation through a Royal Swedish Academy of Sciences fellowship and by NSF CAREER Award No. DMR-0955902. The computations were performed on resources provided by the Swedish National Infrastructure for Computing (SNIC) at National Supercomputer Center at Linkoping, Sweden.

[1] G. E. Volovik, *The Universe in a Helium Droplet* (Oxford University Press, Oxford, UK, 2009); P. W. Anderson and G. Toulouse, Phys. Rev. Lett. **38**, 508 (1977); E. V. Thuneberg, *ibid.* **56**, 359 (1986); M. M. Salomaa and G. E. Volovik, *ibid.* **56**, 363 (1986); Rev. Mod. Phys. **59**, 533 (1987); T. A. Tokuyasu, D. W. Hess, and J. A. Sauls, Phys. Rev. B **41**, 8891 (1990).

[2] J. Jang, D. G. Ferguson, V. Vakaryuk, R. Budakian, S. B. Chung, P. M. Goldbart, and Y. Maeno, Science **331**, 186 (2011).

[3] E. Babaev, Phys. Rev. Lett. **94**, 137001 (2005).

[4] S. B. Chung, H. Bluhm, and E.-A. Kim, Phys. Rev. Lett. **99**, 197002 (2007).

[5] S. B. Chung, D. F. Agterberg, and E.-A. Kim, New J. Phys. **11**, 085004 (2009).
[6] S. B. Chung and S. A. Kivelson, Phys. Rev. B **82**, 214512 (2010).
[7] E. Babaev, J. Jäykkä, and M. Speight, Phys. Rev. Lett. **103**, 237002 (2009).
[8] E. Babaev, Phys. Rev. Lett. **89**, 067001 (2002).
[9] A. Y. Kitaev, Ann. Phys. **303**, 2 (2003).
[10] A. Knigavko and B. Rosenstein, Phys. Rev. Lett. **82**, 1261 (1999); A. Knigavko, B. Rosenstein, and Y. F. Chen, Phys. Rev. B **60**, 550 (1999); B. Rosenstein, I. Shapiro, B. Y. Shapiro, and G. Bel, *ibid.* **67**, 224507 (2003); Q. Li, J. Toner, and D. Belitz, *ibid.* **79**, 014517 (2009); Phys. Rev. Lett. **98**, 187002 (2007).
[11] E. Babaev, Phys. Rev. Lett. **88**, 177002 (2002).
[12] L. F. Chibotaru, V. H. Dao, and A. Ceulemans, Europhys. Lett. **78**, 47001 (2007); L. F. Chibotaru and V. H. Dao, Phys. Rev. B **81**, 020502 (2010); H. Bluhm, N. C. Koshnick, M. E. Huber, and K. A. Moler, Phys. Rev. Lett. **97**, 237002 (2006); R. Geurts, M. V. Milošević, and F. M. Peeters, Phys. Rev. B **81**, 214514 (2010); J. C. Piña, C. C. de Souza Silva, and M. V. Milošević, *ibid.* **86**, 024512 (2012).
[13] E. Babaev, Nucl. Phys. B **686**, 397 (2004); E. Smørgrav, J. Smiseth, E. Babaev, and A. Sudbø, Phys. Rev. Lett. **94**, 096401 (2005).
[14] M. A. Silaev, Phys. Rev. B **83**, 144519 (2011).
[15] D. F. Agterberg, Phys. Rev. Lett. **80**, 5184 (1998).
[16] D. F. Agterberg, Phys. Rev. B **58**, 14484 (1998); R. Heeb and D. F. Agterberg, *ibid.* **59**, 7076 (1999).
[17] See Supplemental Material at http://link.aps.org/supplemental/10.1103/PhysRevB.86.060514 for technical details of numerical calculations.
[18] M. Sigrist and D. F. Agterberg, Prog. Theor. Phys. **102**, 965 (1999); D. G. Ferguson and P. M. Goldbart, Phys. Rev. B **84**, 014523 (2011); V. Vakaryuk, *ibid.* **84**, 214524 (2011).
[19] Y. Matsunaga, M. Ichioka, and K. Machida, Phys. Rev. Lett. **92**, 157001 (2004); Phys. Rev. B **70**, 100502 (2004); M. Ichioka, Y. Matsunaga, and K. Machida, *ibid.* **71**, 172510 (2005).
[20] F. Hecht, O. Pironneau, A. Le Hyaric, and K. Ohtsuka, *The Freefem++ manual*, 2007, www.freefem.org.
[21] E. Babaev, L. D. Faddeev, and A. J. Niemi, Phys. Rev. B **65**, 100512 (2002).
[22] C. W. Hicks, J. R. Kirtley, T. M. Lippman, N. C. Koshnick, M. E. Huber, Y. Maeno, W. M. Yuhasz, M. B. Maple, and K. A. Moler, Phys. Rev. B **81**, 214501 (2010).
[23] J. Garaud, D. F. Agterberg, and E. Babaev, arXiv:1207.6395 [Phys. Rev. B (to be published)].